High efficiency and broadband acoustic diodes

Congyi Fu,[1] Bohan Wang,[1] Tianfei Zhao,[2] and C. Q. Chen[1,a)]
[1]*Department of Engineering Mechanics, CNMM and AML, Tsinghua University, Beijing 100084, People's Republic of China*
[2]*School of Mechanics, Civil Engineering and Architecture, Northwestern Polytechnical University, Xi'an 710072, People's Republic of China*

(Received 26 December 2017; accepted 16 January 2018; published online 29 January 2018)

Energy transmission efficiency and working bandwidth are the two major factors limiting the application of current acoustic diodes (ADs). This letter presents a design of high efficiency and broadband acoustic diodes composed of a nonlinear frequency converter and a linear wave filter. The converter consists of two masses connected by a bilinear spring with asymmetric tension and compression stiffness. The wave filter is a linear mass-spring lattice (sonic crystal). Both numerical simulation and experiment show that the energy transmission efficiency of the acoustic diode can be improved by as much as two orders of magnitude, reaching about 61%. Moreover, the primary working band width of the AD is about two times of the cut-off frequency of the sonic crystal filter. The cut-off frequency dependent working band of the AD implies that the developed AD can be scaled up or down from macro-scale to micro- and nano-scale. *Published by AIP Publishing.*
https://doi.org/10.1063/1.5020698

Acoustic diodes (ADs), diode-like asymmetric transmission devices which permit wave propagation in only one direction, have great potential in medical ultrasound imaging,[1–5] switch and logic gates,[6] isolators,[7,8] wave control,[9] wave demodulation,[10] and phonon control in on-chip devices.[11,12] Among them, subwavelength acoustic diodes are desirable for applications requiring miniaturization of devices.[7,13,14] Asymmetric transmission of acoustic waves usually needs to break either the time-reversal symmetry[1,3,6,7,10,14–18] or the spatial-inversion symmetry.[13,19–25] It has been realized that the reflection-transmission reciprocity can hardly be broken in linear structures.[26] As a result, time-reversal symmetry broken ADs are believed to be more promising for nonreciprocity acoustic devices. To break the time reversibility, numerous methods, such as time-modulation of the parameters,[27–29] odd-vector bias,[7] and strong nonlinearity,[1,3,6,10] have been proposed. Among them, nonlinearity-based broken time-reversal symmetry ADs are one of the most attractive nonreciprocal devices.

A nonlinearity-based time symmetry broken AD normally consists of a nonlinear medium and a sonic crystal (SC) with bandgaps. The nonlinear medium acts as a frequency converter,[10] while the sonic crystal is a wave filter. Within its bandgaps, no wave can propagate. For an ideal AD, high forward energy transmission efficiency and a broad work bandwidth are desirable. However, it is difficult to achieve such an ideal AD.[26] For instance, the transmission efficiency of the first AD which was based on the second harmonic wave is only about 1%.[3] Although a bifurcation-based acoustic rectifier can improve the efficiency to 1.7%,[6] its working band remains to be close to the defect frequency. Recently, it was reported that the self-demodulation effect could broaden the frequency range of the work band, but it hardly improved the energy transmission efficiency.[10] It is still a challenge to have ADs with simultaneous high forward energy transmission efficiency and a wide working band.

In this letter, we propose a method to design ADs consisting of a one-dimensional nonlinear mass-spring system. High energy transmission efficiency and a wide working band are achieved. The design method is validated by numerical simulation and experiment. The developed one-dimensional mass-spring system with a scale-independent structure is beneficial for the future applications on micro- and nano-scale.

As shown schematically in Fig. 1, the AD has two units connected in series, i.e., a frequency conversion unit and a linear frequency filter. The frequency conversion unit is composed of two masses ($m_b = 80$ g) and a tension-compression asymmetrical bilinear spring. The bilinear spring is realized by two springs and a rope as shown in Fig. 1(a). The stiffness of the two springs (k_1 and k_2) are 11.3 N/m and 90.4 N/m, respectively. One of the springs (i.e., k_2) is connected with the rope in series. The rope-spring system is then connected to spring k_1 in parallel. Note that the rope is much stiffer than spring k_2 and can only sustain tensile loading. The resulting system is a tension-compression asymmetrical bilinear spring with tension stiffness $k_T = k_1 + k_2 = 101.7$ N/m and compression stiffness $k_C = k_1 = 11.3$ N/m. The effective natural frequency of the bilinear unit is $f_b = \sqrt{r_b k_C/m}/[\pi(1+\sqrt{r_b})]$,[30] where $r_b = k_T/k_C = 9$ is the asymmetrical stiffness ratio of the bilinear spring. The linear filter comprises N masses ($m = 65$ g) connected by $N-1$ linear springs with stiffness $k = 11.3$ N/m [see, Fig. 1(a)]. When N is sufficiently large, the filter can be treated as a sonic crystal with cutoff frequency $f_c = \sqrt{k/m}/(2\pi) = 4.2$ Hz.[31] Here, $N = 7$ is adopted. For such a sonic crystal, only waves with frequency less than f_c can propagate.

Consider wave propagation in the AD. The driving signal is generated by a vibration exciter (HEV-50N). For the forward wave propagation denoted by "+" in Fig. 1(b), the exciter is placed at the left end of the conversion unit. The time history of the driving and response displacements is

a)Author to whom correspondence should be addressed: chencq@tsinghua.edu.cn

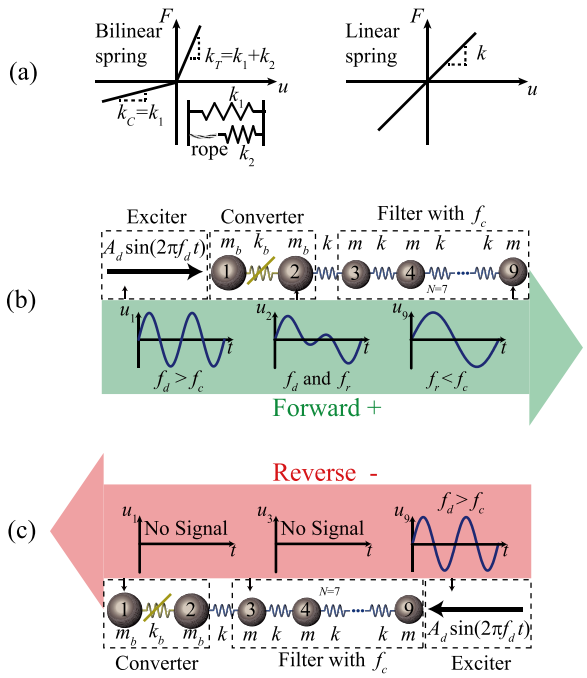

FIG. 1. Schematic of the acoustic diode (AD), consisting of a bilinear frequency converter and a linear sonic crystal (SC) filter with cutoff frequency f_c. (a) The tension-compression asymmetric bilinear and linear springs used in the converter and filter, respectively. The unidirectional propagation of a single frequency harmonic driving wave with frequency $f_d > f_c$ is shown. (b) Forward propagation. The driving wave is modulated by the converter, resulting in an additional subharmonic response wave with frequency $f_r < f_c$. The subharmonic wave can pass through the SC filter. (c) Reverse propagation. The frequency of the driving wave is above the cutoff frequency and lies within the stop band of the SC. It cannot propagate. The stiffness and mass of the AD are marked.

measured with two laser displacement sensors IL-065 and IL-300, respectively. The data record rate is 1000 Hz. When a single frequency harmonic incident wave with $f_d > f_c$ is generated, it is converted into a wave with multi-frequencies (e.g., $f_r, f_d, \ldots$) after passing through the nonlinear conversion unit. Usually, $f_r = \alpha f_d$ with α being greater than 1 for super-harmonic and α being less than 1 for subharmonic.[32] Only the component with $f_r < f_c$ of the converter generated wave can propagate through the sonic crystal filter [as illustrated in Fig. 1(b)]. For the reverse wave propagation denoted by "–" in Fig. 1(c), the same single frequency wave with $f_d > f_c$ is imposed at the right end of the filter. Note that the wave cannot propagate through the filter because its frequency f_d is greater than the cutoff frequency f_c and lies within the stop band of the filter [see, Fig. 1(c)]. As such, the working frequency range of the proposed AD in this letter must satisfy

$$f_c < f_d < f_c/\alpha, \quad \text{with} \quad 0 < \alpha < 1. \tag{1}$$

Theoretically, smaller α indicates a wider working band in frequency. However, the transmitted wave energy is usually proportional to $(A_r \alpha f_d)^2$ with A_r being the response amplitude. For higher energy transmission efficiency, large α is desirable. Therefore, there is a trade-off in α. Usually, the primary 1/2-order subharmonic waves carry the most significant amount of energy and $\alpha = 1/2$ is of most interest in this letter. A design method of the AD is proposed in the following. The method relies on the wave propagation property of the frequency converter and the sonic crystal.

The numerically simulated and experimentally measured frequency responses of the conversion unit to a harmonic driving displacement $A_d \sin(2\pi f_d t)$ are presented in Figs. 2(a)–2(c), where A_d and f_d are the amplitude and frequency, respectively. Due to the nonlinearity of the conversion unit, a single frequency driving signal can produce a multi-frequency response wave. This can be seen from Fig. 2(a) which shows a typical displacement amplitude A_r-frequency f_r response of the converter to sinusoidal driving displacement with $A_d = 2$ mm and $f_d = 1.9 f_b = 5.4$ Hz, where the response displacement amplitude is normalized by A_d. It should be emphasized that, owing to the characteristic feature of the bilinear spring, the results and conclusions are not dependent on the particular choice of A_d adopted in the simulations. The simulation method can be found in the supplementary material with the damping factor of 4% in order to match the measurement. It is clear from the experiments and simulations that both subharmonic (e.g., $f_r = 1/2 f_d$) and super-harmonic (e.g., $f_r = 2 f_d$) responses are presented. By varying the driving frequency f_d, contours of the normalized response displacement amplitude can be obtained in the driving frequency-response frequency space, as shown in Figs. 2(b) and 2(c) for the experimental and numerical results, respectively, where the order of the harmonic response is marked. The results show that, when the driving signal satisfies $f_d/f_b > 1$, most energy is transferred to the lowest subharmonic components, as marked by the open ellipses. It should be pointed out that there is a discrepancy between Figs. 2(b) and 2(c), in that the 1/4-order subharmonic wave in the experiment is shifted to the 1/3-order subharmonic wave in

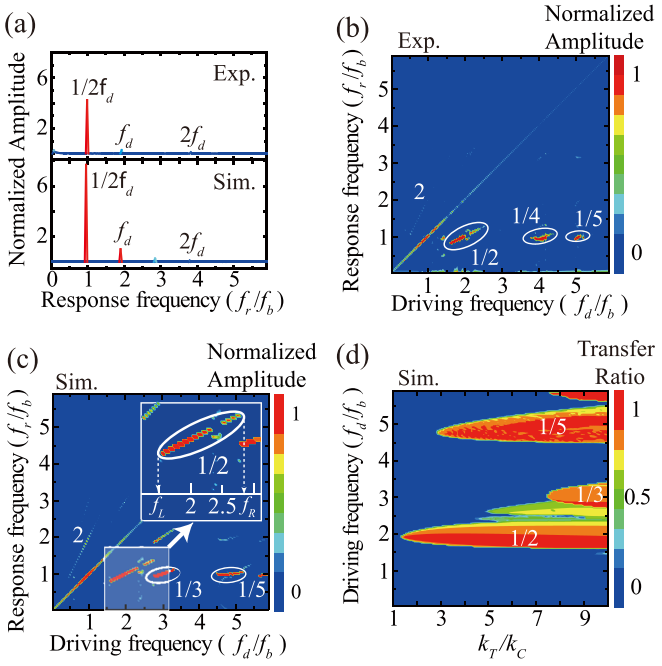

FIG. 2. The frequency responses of the bilinear converter. (a) Experimental and numerical results of the normalized amplitude-frequency response of the converter to a single frequency harmonic driving signal with $f_d = 1.9 f_b$, where f_b is the effective natural frequency of the converter. (b) Experimental and (c) numerical contours of the normalized amplitude of the response in the driving-response frequency space. (d) Contours of the numerically simulated energy transfer ratio of the converter in the asymmetric stiffness ratio-driving frequency space. In (a)-(c), the asymmetric stiffness ratio is $r_b = k_T/k_C = 9$.

simulation. One possible reason is that the bilinear spring in the experiment is not ideal.

A transfer ratio of the conversion unit can be defined to quantify the ratio of the energy at the lowest subharmonic frequency to the whole energy. Figure 2(d) shows the numerical simulated transfer ratio as a function of the driving frequency and the asymmetric stiffness ratio. As a rule of thumb, the converter can be regarded to be energy efficient when its transfer ratio is greater than 50%. The results in Fig. 2(d) show that for small values of α, the high energy transfer ratio regime is narrow. In particular, when α approaches 1, the bilinear spring becomes a linear one, resulting in neither subharmonic nor super-harmonic responses. Accordingly, the transfer ratio is 0. With increasing α, the high energy transfer ratio regime of the primary 1/2-order subharmonic waves widens and gradually approaches a constant value for α greater than about 7 for the considered range in Fig. 2(d). Although larger α can be simulated, it is difficult to realize in the experiment a bilinear spring with a very large value of α. Note that for an AD with high efficiency and a wide working frequency range, the conversion unit should have a high transfer ratio in a wide frequency range. According to Fig. 2(d), a bilinear spring with $\alpha > 7$ can be regarded as an optimal design, at least as a first order approximation.

To design an AD with the bilinear converter and the linear sonic crystal filter connected in series, their coupling effect must be considered. As a conceptual demonstration, we show in the following how to design the filter for the converter given in Fig. 2(c) with $r_b = 9$. For simplicity, only the primary 1/2-order subharmonic wave of the converter is considered in the design. Denote the driving frequency range for the primary 1/2-order subharmonic wave with a high transfer ratio response by $f_L < f_d < f_R$, where f_L and f_R are illustrated in Fig. 2(c) for a given r_b. To ensure unidirectional wave propagation [i.e., Eq. (1) with $\alpha = 1/2$] and high energy transmission efficiency of the AD, the cutoff frequency of the sonic crystal filter should be in the range given by

$$f_R/2 < f_c < f_L. \tag{2}$$

For the case $r_b = 9$ given by Fig. 2(c), $f_L = 4.3$ Hz and $f_R = 7.7$ Hz. Accordingly, Eq. (2) gives 3.85 Hz $< f_c <$ 4.3 Hz. Note that the cutoff frequency of the sonic crystal filter in the designed AD given in Fig. 1 is 4.2 Hz and satisfies the condition.

The forward and reverse wave propagations of the AD are investigated experimentally [Movie 3(a) (Multimedia view) shows the wave propagations in forward and reverse] and numerically. Details of the numerical simulations can be found in the supplementary material. The experimental setups are given in Fig. 3(a) (Multimedia view) where the slide blocks are put on top of an air track to minimize the friction. The orange blocks constitute the tension-compression asymmetrical bilinear converter, while the blue ones belong to the sonic crystal filter. A harmonic driving signal is generated by the exciter. The energy transmission is quantified by the ratio of the time-averaged kinetic energy of the last response slide block to that of the first driving block.[6] Experimental and numerical results of the forward and reverse wave propagation are plotted in Figs. 3(b) and 3(c), respectively, where the shaded regions denote the frequency working bands for unidirectional wave propagation and their associated energy transmission ratios are labeled. From the experimental results, it is evident that, when the normalized driving frequency is between 1 and 2, unidirectional wave propagation is realized, consistent with the primary 1/2-order subharmonic prediction in Eq. (1). Additional unidirectional wave propagation is also observed from the experiment in the range $2.35 < f_d/f_c < 3.15$, which is in fact due to the secondary lower order subharmonic waves (e.g., 1/3- and 1/5-order subharmonic waves). However, the transmission efficiency associated with the secondary working band is much lower.

The experimental results in Fig. 3(b) also show that the working band width of the AD is at least the same as the cut-off frequency if only the primary unidirectional transmission is considered or even greater than the cut-off frequency if the secondary unidirectional transmissions are taken into account. Most importantly, the average energy transmission efficiency of the primary working band is about 61% which is one to two orders of magnitude higher than that of previous ADs with an energy transmission efficiency of only about 1%.[3,6,10] Figure 3(c) shows the corresponding numerical simulations of the energy transmission of the experimental systems given in Fig. 3(a) (Multimedia view). A comparison between Figs. 3(b) and 3(c) shows good overall agreement between the experimental and numerical results. It is noted that the experimental results show a slightly narrower primary working band width and lower transmission efficiency. The differences are possibly due to the idealized bilinear model and the uncertainty of the damping effect in the simulation, which also indicate that the designed real AD has room for improvement.

In conclusion, an acoustic diode consisting of a tension-compression asymmetric bilinear frequency converter and a linear sonic crystal wave filter is developed. The proposed design method is demonstrated by simulations and experiments. Much improved primary energy transmission efficiency (61%) and a wide working width in frequency

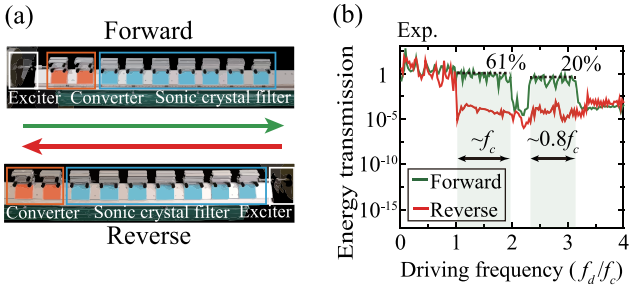

FIG. 3. (a) Screenshots of the forward and reverse wave propagation in the AD. Experimental (b) and simulated (c) results of the forward and reverse energy transmissions as a function of the driving frequency. The shaded regions denote unidirectional wave propagation. Multimedia view: https://doi.org/10.1063/1.5020698.1

(i.e., $2f_c$) are achieved. Owing to the bilinear feature of the converter, the unidirectional wave propagation is independent of the amplitude of the driving signal. Moreover, the frequency working width of the AD is governed by the cutoff frequency f_c of the sonic crystal filter. These properties indicate that the AD can be scaled up or down from macro-scale to micro- and nano-scale devices. It is also noted that the developed AD can be made tunable if the asymmetric stiffness ratio of the bilinear spring can be changed during in-life service.

See supplementary material for details of numerical simulation.

The authors are grateful for the financial support by the National Natural Science Foundation of China (Nos. 11732007, 11472149, and 11402201).

[1]B. Liang, B. Yuan, and J. C. Cheng, Phys. Rev. Lett. **103**, 104301 (2009).
[2]B. Liang, X. Y. Zou, B. Yuan, and J. C. Cheng, Appl. Phys. Lett. **96**, 233511 (2010).
[3]B. Liang, S. S. Guo, J. Tu, D. Zhang, and J. C. Cheng, Nat. Mater. **9**, 989 (2010).
[4]C. H. Li, M. Z. Ke, Y. T. Ye, S. J. Xu, C. Y. Qiu, and Z. Y. Liu, Appl. Phys. Lett. **105**, 023511 (2014).
[5]X. P. Wang, L. L. Wan, T. N. Chen, Q. X. Liang, and A. L. Song, Appl. Phys. Lett. **109**, 044102 (2016).
[6]N. Boechler, G. Theocharis, and C. Daraio, Nat. Mater. **10**, 665 (2011).
[7]R. Fleury, D. L. Sounas, C. F. Sieck, M. R. Haberman, and A. Alù, Science **343**, 516 (2014).
[8]D. L. Sounas and A. Alù, Phys. Rev. Lett. **118**, 154302 (2017).
[9]Y. Li, C. Shen, Y. B. Xie, J. F. Li, W. Q. Wang, S. A. Cummer, and Y. Jing, Phys. Rev. Lett. **119**, 035501 (2017).
[10]T. Devaux, V. Tournat, O. Richoux, and V. Pagneux, Phys. Rev. Lett. **115**, 234301 (2015).
[11]M. B. Zanjani, A. R. Davoyan, A. M. Mahmoud, N. Engheta, and J. R. Lukes, Appl. Phys. Lett. **104**, 081905 (2014).
[12]M. B. Zanjani, A. R. Davoyan, N. Engheta, and J. R. Lukes, Sci. Rep. **5**, 9926 (2015).
[13]S. Zhang, Y. Zhang, Y. J. Guo, Y. H. Leng, W. Feng, and W. W. Cao, Phys. Rev. Appl. **5**, 034006 (2016).
[14]B. I. Popa and S. A. Cummer, Nat. Commun. **5**, 3398 (2014).
[15]S. Lepri and G. Casati, Phys. Rev. Lett. **106**, 164101 (2011).
[16]N. Bender, S. Factor, J. D. Bodyfelt, H. Ramezani, D. N. Christodoulides, F. M. Ellis, and T. Kottos, Phys. Rev. Lett. **110**, 234101 (2013).
[17]N. B. Li and J. Ren, Sci. Rep. **4**, 6288 (2014).
[18]J. Zhang, B. Peng, Ş. K. Özdemir, Y. X. Liu, H. Jing, X. Y. Lü, Y. L. Liu, L. Yang, and F. Nori, Phys. Rev. B **92**, 115407 (2015).
[19]X. F. Li, X. Ni, L. Feng, M. H. Lu, C. He, and Y. F. Chen, Phys. Rev. Lett. **106**, 084301 (2011).
[20]Z. J. He, S. S. Peng, Y. T. Ye, Z. W. Dai, C. Y. Qiu, M. Z. Ke, and Z. Y. Liu, Appl. Phys. Lett. **98**, 083505 (2011).
[21]A. Cicek, O. Adem Kaya, and B. Ulug, Appl. Phys. Lett. **100**, 111905 (2012).
[22]H. X. Sun, S. Y. Zhang, and X. J. Shui, Appl. Phys. Lett. **100**, 103507 (2012).
[23]Y. Li, J. Tu, B. Liang, X. S. Guo, D. Zhang, and J. C. Cheng, J. Appl. Phys. **112**, 064504 (2012).
[24]S. Alagoz, Appl. Acoust. **76**, 402 (2014).
[25]B. Y. Xie, H. Cheng, K. Tang, Z. Y. Liu, S. Q. Chen, and J. G. Tian, Phys. Rev. Appl. **7**, 024010 (2017).
[26]A. A. Maznev, A. G. Every, and O. B. Wright, Wave Motion **50**, 776 (2013).
[27]Q. Wang, Y. Yang, X. Ni, Y. L. Xu, X. C. Sun, Z. G. Chen, L. Feng, X. P. Liu, M. H. Lu, and Y. F. Chen, Sci. Rep. **5**, 10880 (2015).
[28]P. A. Deymier, V. Gole, P. Lucas, J. O. Vasseur, and K. Runge, Phys. Rev. B **96**, 064304 (2017).
[29]C. Croënne, J. O. Vasseur, O. Bou Matar, M. F. Ponge, P. A. Deymier, A. C. Hladky-Hennion, and B. Dubus, Appl. Phys. Lett. **110**, 061901 (2017).
[30]Y. C. Chu and M. H. Shen, AIAA J. **30**, 2512 (1992).
[31]P. A. Deymier, *Acoustic Metamaterials and Phononic Crystals* (Springer Science & Business Media, 2013), Vol. 173.
[32]Z. K. Peng, Z. Q. Lang, S. A. Billings, and Y. Lu, Int. J. Mech. Sci. **49**, 1213 (2007).